Korean J. Chem. Eng., 37(9), 1565-1572 (2020)
DOI: 10.1007/s11814-020-0540-3

pISSN: 0256-1115
eISSN: 1975-7220

Optimization of heat exchanger network in the dehydration process using utility pinch analysis

Moon Jeong*, Seon Gyun Rho, Choon-Hyoung Kang***,†, and In Ju Hwang****,†**

*Department of Chemical & Industrial Eng., Hanyeong University, Yeosu-si, Jeollanam-do 59720, Korea
**Department of Fire Service Admin., Honam University, Gwangju 62399, Korea
***School of Chem. Eng., Chonnam National University, Gwangju 61186, Korea
****Korea Institute of Civil Eng. and Building Tech., Goyang-si, Gyeonggi-do 10223, Korea
(*Received 3 December 2019 • Revised 10 March 2020 • Accepted 13 March 2020*)

Abstract−Pinch analysis was applied to optimize the heat exchange network used in the moisture removal processes of energy plants. The moisture removal process absorbs moisture from natural gas using glycol as an absorbent, and the recycling process then separates moisture from the H_2O-rich glycol in a regenerator column by applying the principle of vapor-liquid equilibria. For the dehydration process of a natural gas plant, the heat and mass flows are properly established and calculated by means of a static process model for a utility system embedded in the process based on the properties of natural gas. The results of the calculation generate a T-H composite curve that can be used to compare the pinch and to assess the installation and operating costs for the target temperature. The results show that approximately 61% of the total heat supply can be replaced with low-pressure steam, depending on the optimization of the heat exchanger network of the moisture removal process. Further, the annual operating costs can be reduced by about 17% in this case.

Keywords: Dehydration Process, Heat Exchanger Network, Pinch Analysis, Plant Engineering, Cold Region

INTRODUCTION

Numerous energy plants that consist of several processing stages have been devoting a huge amount of their efforts to improving the efficiency of their systems and reducing greenhouse gases emission. These plants are increasing in size and becoming more sophisticated, so there is greater interest in reducing operating costs and maximizing heat conduction [1,2].

Most large plants that use various complex heat exchange networks utilize exergy theory, pinch analysis, mathematical programming, or stochastic optimization to optimize the processing systems [3-5]. Linnhoff et al. [6] explained complex mathematical methods that are involved in heat exchange network design via the pinch analysis with a pictorial overview and provided insight into the concept of composite and network curves. However, large-scale plants that did not operate in a unit process could not use Linnhoff's design and showed limitations in the analysis of heat exchange processes. Ebrahim et al. [7] showed that the pinch analysis method has been used for over 20 years since its introduction and reported the results in terms of energy reduction, a decrease in the initial investment fee, and the effective operation of heat exchange networks in the industry. Geldermann et al. [8] incorporated the pinch analysis method into an integrated process design to reduce the operating costs. Furthermore, they designed an effective heat exchange method with the corresponding network for plants using a solvent to process automobile surfaces and dehydration operations. The pinch analysis method was used to integrate various heat exchange systems, leading to a reduction in the operating costs and an improvement on their efficiency [9]. Smith et al. [10] combined Linnhoff's pinch method and a complex mathematical programming method to improve the heat exchange system in crude oil distillation process. The results showed an overall reduction of almost 23% in energy. Moreover, they found that the pinch method could be improved by combining it with a complex mathematical programming method to optimize a large-scale plant operating system.

Typically, when a conventional heat exchange system is analyzed by using the pinch method, heat transfer occurs between hot fluids above the pinch point while heat transfer between cold fluids occurs below the pinch point. The accurate placement of heat exchangers in a system eliminates the additional cross-pinch heat exchangers in the system, and energy production becomes closer to the target production [11,12]. Yoon et al. [13] used the pinch method to improve heat exchange networks in plants that use ethylbenzene and found that the total annual cost could be reduced by 5.6% by improving the heat exchanger in the distillation process. Furthermore, the reduction in operating costs was more drastic than the cost incurred in improving the actual processing system. Tuan et al. [14] implemented the pinch method to improve the production processing stages for a gelatin-based three-effect evaporator. Two cases were considered for the improvement: first, a simple enhancement of the heat exchange network by implementing the pinch method, and second, the installation of additional heat pumps in the system and also implementing the pinch method. The results showed that applying the pinch method to an existing operational system

†To whom correspondence should be addressed.
E-mail: chkang@jnu.ac.kr, ijhwang@kict.re.kr

was sufficient without additional pumps.

This study applied pinch analysis to the dehydration process of liquefied natural gas (LNG) plants using triethylene glycol (TEG, $C_6H_{14}O_4$) to improve the heat transfer efficiency. In this effort, the pinch point on a composite curve was optimized to obtain the outer limit for an overall improvement in the heat exchange networks of various energy plants.

ANALYSIS MODEL AND METHOD

1. Moisture Removal Process

The pretreatment for natural gas liquefaction consists of sweating and dehydration processes, as shown in Fig. 1, to remove impurities (including carbon dioxide and sulfur) and moisture from gas by using absorbents such as amine and glycol to stabilize the subsequent liquefaction process. Removing moisture from natural gas in a dehydration process prevents corrosion and mechanical damage of equipment that may result from the formation of hydrates.

The dry natural gas resulting from pretreatment processes is then cooled and liquefied in a subsequent liquefaction process that utilizes propane and refrigerant mixtures. Further, the fractionation process of the natural gas results in ethane, propane, butane, and others, and nitrogen is then freed in the following step.

The moisture removal process indicated by the dotted line in Fig. 1 consists of two systems: the supply system of natural gas containing moisture and the supply system of glycol that absorbs and removes moisture. As shown in Fig. 2, the introduced wet gas containing moisture is discharged through the dry gas outlet after its moisture is removed by glycol in the contactor tower. In general, the rich glycol that absorbs moisture from natural gas is heated to 100-110 °C in the heat exchange with lean glycol, and it is supplied to the regenerator column. This stream is then flashed, resulting in the formation of the H_2O-rich gas phase and the solvent-rich liquid phase on basis of the principle of the vapor-liquid equilibrium. Subsequently, the H_2O-rich gas phase is released through the vapor outlet, and the solvent-rich liquid phase is heated to 200-210 °C

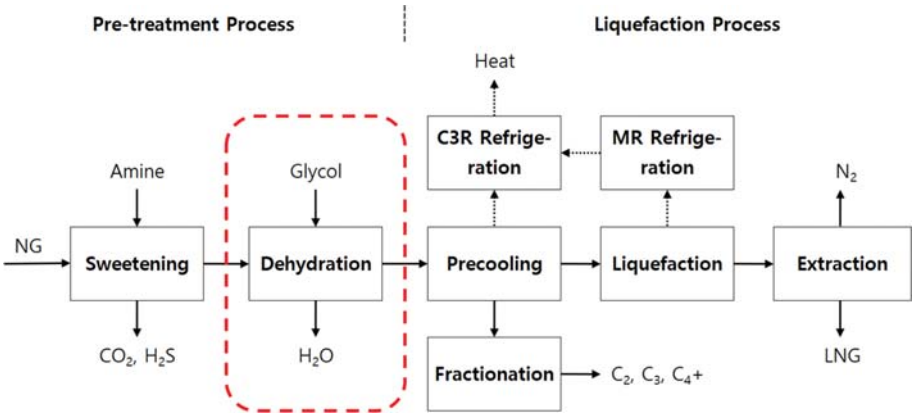

Fig. 1. Schematic diagram of the liquefied natural gas plant.

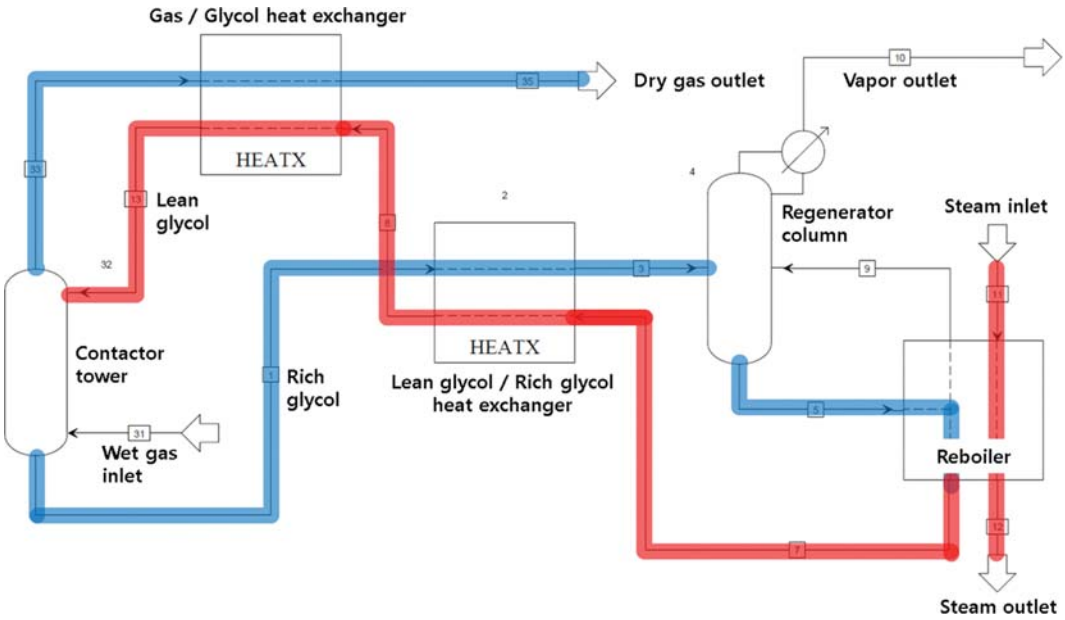

Fig. 2. Typical flow diagram for a glycol dehydration process.

Table 1. Properties and composition of natural gas

Properties			Composition		
Name	Unit	Value	Name	Formula	[mol%]
Vapor fraction	-	1.0000	Nitrogen	N_2	4.98
Mole flow	kmol/h	271.2	Methane	CH_4	87.06
Mass flow	kg/h	4,972.9	Ethane	C_2H_6	5.07
Enthalpy	10^6 W	0.2	Propane	C_3H_8	1.98
Entropy	kcal/kg·K	2.4	i-Butane	C_4H_{10}	0.44
MW	kg/kgmol	18.33	n-Butane	C_4H_{10}	0.45
Pressure	bar_a	70.0	i-Pentane	C_5H_{12}	0.01
Temperature	°C	15.0	n-Pentane	C_5H_{12}	0.01

with help of the regeneration steam in the reboiler. The liquid phase, which consists of H_2O-lean glycol, is cooled to approximately 50 °C by using the rich glycol, and then the dry gas from the contact tower in succession before it is recycled to the contactor tower to absorb the moisture from natural gas [15].

Table 1 shows the composition of the natural gas used in this study. The Peng-Robinson equation of state (PR-EOS) [16] is widely applicable to hydrocarbon-based phase equilibrium calculations under a wide range of temperature and pressure conditions. Thus, the PR-EOS was used to obtain the enthalpy required to calculate the heat engine efficiency and the power for closure of the heat and material balances in this work.

Briefly, PR-EOS is given by

$$P = \frac{RT}{V-b} - \frac{a(T)}{V(V+b)+b(V-b)} \quad (1)$$

The parameters a and b are as follows.

$$a(T) = 0.45724\frac{(RT_c)^2}{P_c}\alpha(T_r, \omega)$$

$$b = 0.07780\frac{RT_c}{P_c}$$

$$\alpha(T_r, \omega) = [1+(0.37464+1.54226\omega-0.26992\omega^2)(1-T_r^{1/2})]^2$$

where T_r and P_r are the reduced temperature and pressure, respectively, and ω is the acentric factor suggested by Pitzer [17].

This work configured and analyzed the heat exchanger network by using Aspen HYSYS, Aspen Energy analyzer, and their built-in parameters extensively.

2. Pinch Analysis

The pinch analysis is a method that minimizes the energy consumption of a relevant process by calculating a thermodynamically feasible energy target (minimum energy consumption) and by optimizing the bootstrap system, energy supply method, and process operating conditions to reach the target. It is also referred to as process integration, heat integration, energy integration, or pinch technology [18].

The T-H composite curve in the pinch analysis combines hot streams that release heat into one stream and cold streams that absorb heat from another stream and represents them on one graph that shows the change in the enthalpy change (y-axis) with temperature (x-axis). In addition, the pinch analysis uses the grand composite curve, which represents the changes in heat supply and demand within the process. In addition, it is possible to examine the amount of heat exchange between an external utility and the process flow by using a balance curve, in which a utility stream is added to the composite curve.

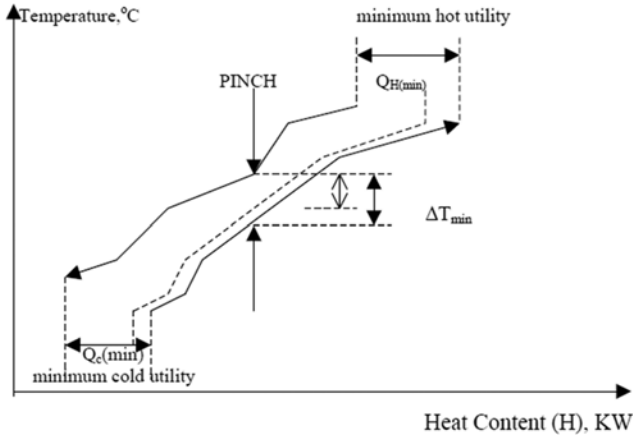

Fig. 3. Energy targets and pinch with composite curves.

As shown in Fig. 3, the point where the vertical distance between the hot stream composite curve and cold stream composite curve is minimized is referred to as the "pinch point," and the temperature of this point is referred to as the "pinch temperature." The temperature that can reach the energy target (ΔT_{min}) must be determined between the hot and the cold stream composite curves in a system that is vertically separated by the pinch point.

The procedure for the pinch analysis is as follows. First, hot, cold, and utility flows are identified in the chemical process, and the temperature, specific heat, and enthalpy data are extracted from each flow. Second, after the minimum approach temperature difference (ΔT_{min}) is set, the composite curve and the grand composite curve are created. Third, the minimum energy consumption is calculated by performing energy targeting. Fourth, the minimum approach temperature difference is determined so that the total cost of the equipment (capital cost) and energy cost can be minimized. Finally, a heat exchange network is designed on the grid curve, which is improved using the pinch method.

3. Estimation Equation for the Yearly Operating Cost

The energy cost and capital cost are calculated to examine eco-

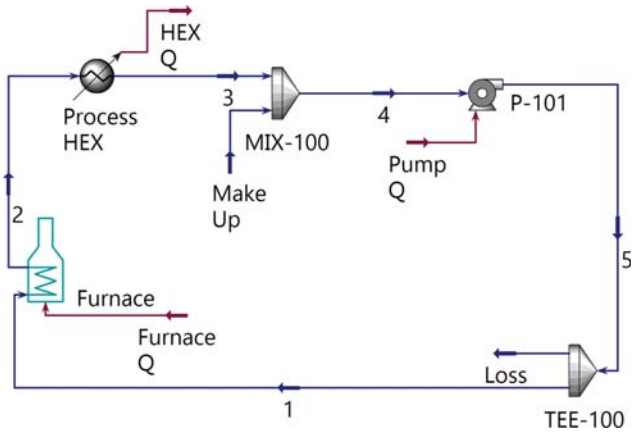

Fig. 4. Process flow diagram of the utility process. Furnace Q: Furnace heat duty, HEX: Heat exchanger, HEX Q: Process heat duty, MIX: Mixer, P: Pump, Pump Q: Pump power, TEE: Three effect evaporator.

nomic validity using the results of the energy targeting obtained through the pinch analysis.

The energy cost excludes charges such as taxes and maintenance expenses from the operating costs. It evaluates the minimum utility of the hot and cold streams corresponding to the target temperature difference (ΔT_{min}) derived through the optimization of the heat exchange network of the moisture removal process on the composite curve. The energy cost is calculated as shown in Eq. (2),

Table 2. Utility cost index

Steam	Cost [$/kcal]
HP (250 °C, 50 bar)	9.804e-5
MP (175 °C, 15 bar)	8.221e-5
LP (125 °C, 5 bar)	6.829e-5

based on the unit energy cost.

$$E{\cdot}C=\Sigma(C_h\times Q_{h,min})+\Sigma(C_c\times Q_{c,min}) \quad (2)$$

where E·C is the energy cost, C_h and C_c are the utility costs of the high and low temperatures, respectively. $Q_{h,min}$ and $Q_{c,min}$ represent the energy target values (kW) of the high and low temperatures.

The production cost of the utility used in the moisture removal process per unit calorie is estimated based on the power plant process shown in Fig. 4 and the results are summarized in Table 2. In calculating this production cost, the cost of anthracite, which is the fuel of the heating furnace, is set to 0.0318 won/kcal, and the electricity cost of the pump is set to 88.76 won/kWh. The loss at TEE-100 is assumed to be 1%.

The initial investment is the cost of the installation of the heat exchange network constructed to supply the minimum utility of the hot and cold streams corresponding to the derived energy target temperature (ΔT_{min}), and it is calculated as given by Eq. (3).

$$C\cdot C=a+b\times\left(\frac{\text{Area}}{\text{Shells}}\right)^{c}\times\text{Shells} \quad (3)$$

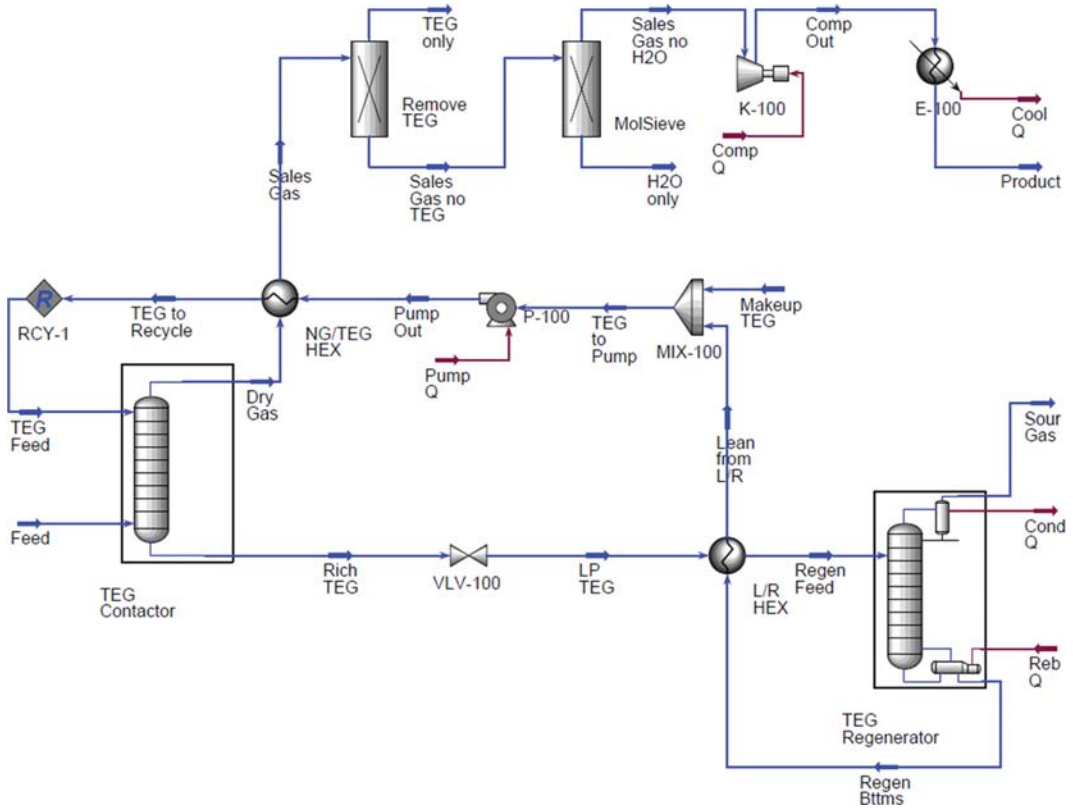

Fig. 5. Process flow diagram of the dehydration process. VLV: Valve, HEX: Heat exchanger, MIX: Mixer, P: Pump, Pump Q: Pump power, K: Compressor, Comp Q: Compressor power, E: Cooler, Cool Q: Cooler duty, Cond Q: Condenser duty, Reb Q: Reboiler duty.

where C.C is the initial investment cost, *a* is the installation cost of the heat exchanger, and b and c are the duty/area-related cost set coefficients of the heat exchanger. Area and Shells are the heat transfer area of the heat exchanger and the number of heat exchanger shells, respectively [13,19].

The total annual cost is calculated by substituting Eqs. (2) and (3) into Eq. (4).

$$T.A.C=A\times\Sigma(C\cdot C+E\cdot C) \quad (4)$$

Here, A is given by

$$A=\frac{\left(1+\frac{ROR}{100}\right)^{PL}}{PL} \quad (5)$$

where T.A.C. is the total annual cost, A is the annualization factor, ROR is the rate of return, which is the investment capital recovery rate and is fixed at 10%, and PL is the plant life, which is the service life of the plant heat exchanger network and is assumed to be 15, 20, or 25 years.

RESULTS

Fig. 4 presents the definition of the hot stream and cold stream flows for the moisture removal process, and the static process model for the moisture removal process and utility system was constructed as shown in Fig. 5. In addition, the heat and material balances were calculated based on the material properties of natural gas, as presented in Table 1 [20]. The utility cost index is shown in Table 2 and the results are summarized in Table 3.

In Fig. 5, 'Feed' (30 °C, 6,200 kPa, 4,981 kg/h) indicates the flow of natural gas including carbon dioxide and sulfur, which are removed in the amine treater. In TEG Contactor, which is the contactor tower, the moisture contained in Feed is removed by means of TEG. In addition, the remaining trace amounts of TEG and moisture (H_2O) are removed in Remove TEG and MolSieve, respectively. This sweetened and dehydrated gas flow resulting from this process is then directed to a subsequent liquefaction process.

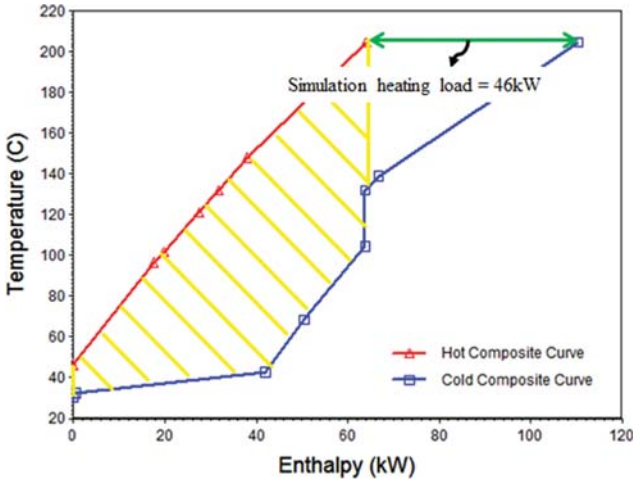

Fig. 6. T-H composite curve.

The TEG feed (50 °C, 6,205 kPa, 563 kg/h) absorbs moisture from the feed flow in TEG Contactor, and rich TEG (27 °C, 6,205 kPa, 285 kg/h), which contains the absorbed moisture, is supplied to TEG Regenerator after heating to 105 °C in L/R HEX (heat exchanger). Regen Bttms (205 °C, 103 kPa, 563 kg/h), which is a regenerated absorbent by dehydration in TEG Regenerator, is cooled to 50 °C in L/R HEX and NG/TEG HEX in succession. This stream is then directed to TEG Contactor after being pressurized to 6,205 kPa by the P-100 pump.

Based on these results, the T-H composite curve and grand composite curve, respectively, presented in Figs. 6 and 7, were created to compare the pinch. In these figures, the areas with deviant crease lines represent the areas for which the amount of heat was gained or lost between the hot streams and cold streams in the heat exchange. The hot and cold composite curves in Fig. 6, respectively,

Table 3. Heat/Material balance of the hydration process

Name	Feed	Dry gas	Product	TEG feed	Rich TEG	Sour gas	Regen bttms
Vapor fraction	1.0000	1.0000	1.0000	0.0000	0.0000	1.0000	0.0000
Temperature [°C]	30.00	32.61	43.40	50.00	30.78	102.00	205.00
Pressure [kPa]	6200	6190	6155	6205	6200	101	103
Mole flow [kmol/h]	271.63	271.27	271.26	4.01	4.37	0.36	4.01
Heat flow [kJ/h]	−2.0e+7	−2.0e+7	−2.0e+7	−3.0e+6	−3.1e+6	−6.3e+4	−2.8e+6
Enthalpy [kJ/kmol]	−7.4e+4	−7.4e+4	−7.3e+4	−7.5e+5	−7.1e+5	−1.7e+5	−7.0e+5
Nitrogen [mol%]	0.0497	0.0497	0.0497	0.0000	0.0062	0.0747	0.0000
Methane [mol%]	0.8681	0.8689	0.8690	0.0000	0.0185	0.2240	0.0000
Ethane [mol%]	0.0510	0.0510	0.0510	0.0000	0.0032	0.0384	0.0000
Propane [mol%]	0.0213	0.0213	0.0213	0.0000	0.0022	0.0271	0.0000
i-Butane [mol%]	0.0044	0.0044	0.0044	0.0000	0.0002	0.0025	0.0000
n-Butane [mol%]	0.0045	0.0045	0.0045	0.0000	0.0002	0.0029	0.0000
i-Pentane [mol%]	0.0001	0.0001	0.0001	0.0000	0.0000	0.0000	0.0000
n-Pentane [mol%]	0.0001	0.0001	0.0001	0.0000	0.0000	0.0001	0.0000
TEG [mol%]	0.0000	0.0000	0.0000	0.9262	0.8498	0.0006	0.9262
H_2O [mol%]	0.0009	0.0001	0.0000	0.0738	0.1197	0.6297	0.0738

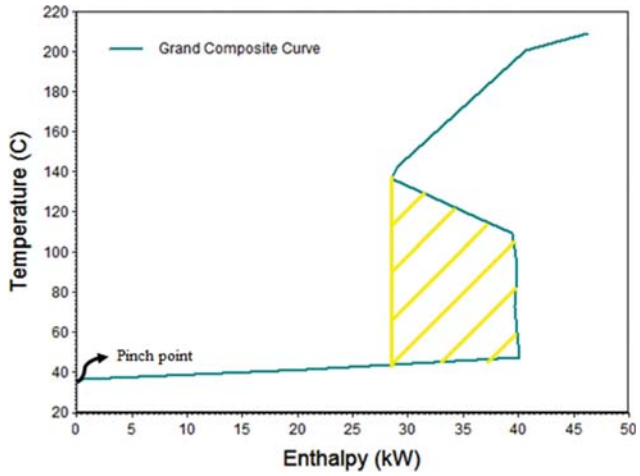

Fig. 7. T-H grand composite curve.

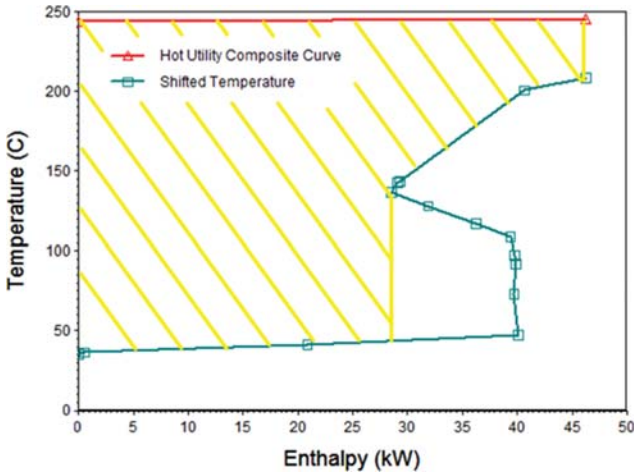

Fig. 9. Utility composite curve with one utility.

represent the removed and added heat flows in the heat exchange.

The grand composite curve in Fig. 7 shows the hot and cold stream composite curves from Fig. 6 on the T-H composite curve. Fig. 7 shows the area where heat is exchanged between the hot streams and the cold streams and the area where heat is exchanged with the utility along with the amount. This figure becomes the basis for the selection of the utility, and the analysis in Figs. 6 and 7 confirms that no utility is required below the pinch point (cooling) while approximately 46 kW of utility is required above the pinch point (heating).

The balanced composite curve and the utility composite curve obtained by adding high-pressure steam heating (250 °C, 5,000 kPa) utility to the composite curves in Figs. 6 and 7 are presented in Figs. 8 and 9, respectively. In these figures, the areas with deviant crease lines represent the heat duty of the utility and the amount of heat exchange between the hot streams and cold streams occurring in the heat exchange. The results show that the amount of heat that is exchanged increases with the area of the deviant crease lines, and the energy cost also increases accordingly. To minimize the energy cost, also on a basis of the results, it is advisable to reduce the differences between the heat exchange temperatures using several levels of low-level utilities.

To investigate the possibility of replacing the high-pressure steam used in Fig. 9 with medium-pressure steam (175 °C, 1,500 kPa) or low-pressure steam (125 °C, 500 kPa), the balance composite curves and utility composite curves were obtained by setting the minimum approach temperature difference to 8.5 °C with various grades of steam (i.e., high-pressure, medium-pressure, and low-pressure steam) as a heat source. Based on the resulting curves shown in Figs. 10 and 11, approximately 102.9 MJ/h (61%) and 21 MJ/h (13%) could be replaced by low-pressure steam and medium-pressure steam, respectively, which corresponds to approximately 74% of the total heat supply. However, since the area that could be replaced with the medium-pressure steam is only 13% of the total heat supply, adding only low-pressure steam as a heat source was deemed to be effective considering the installation cost. Taking into account this result, the balance composite curve and the grand composite curve obtained by using high-pressure steam or low-pressure steam as a heat source were constructed as shown in Figs. 12 and 13, respectively. These results are used to conjecture that the process

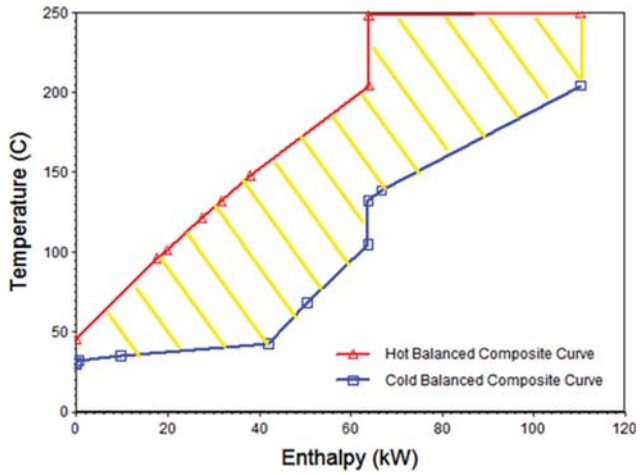

Fig. 8. Balanced composite curve with one utility.

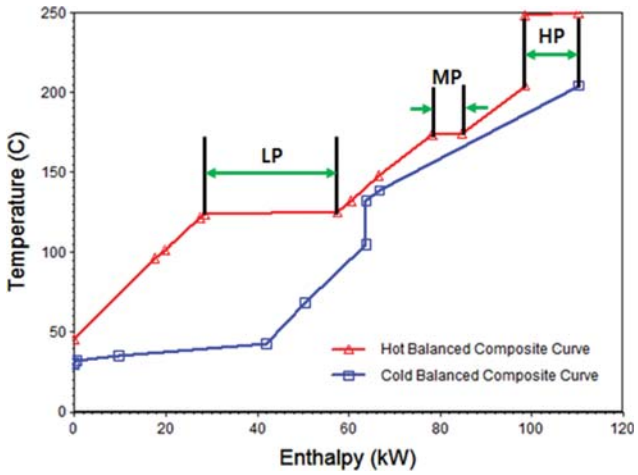

Fig. 10. Balanced composite curve with three utilities.

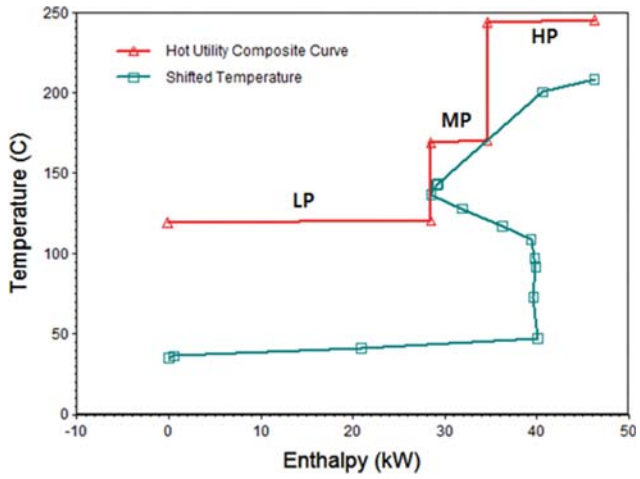

Fig. 11. Utility composite curve with three utilities.

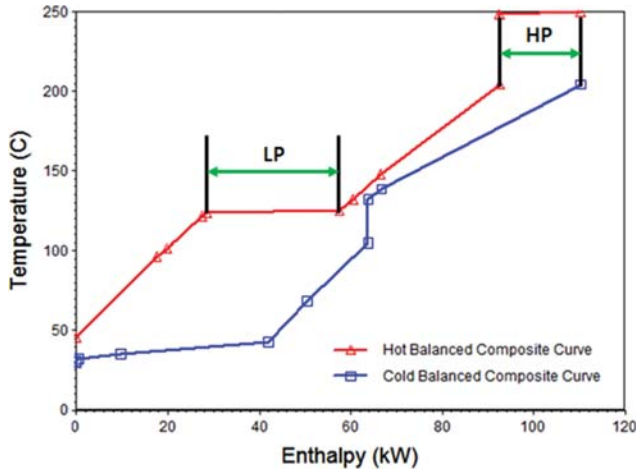

Fig. 12. Balanced composite curve with two utilities.

may be modified as shown in Fig. 14 to optimize the process in the aspect of energy efficiency. That is, a heat exchanger is installed in the Rich TEG-Regen Feed flow to supply heat from the low-

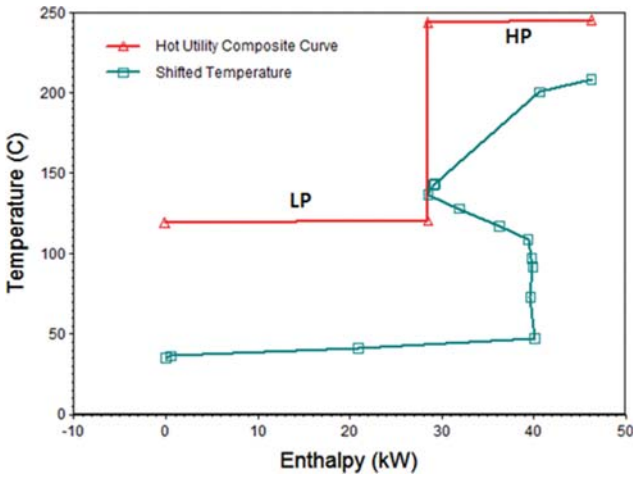

Fig. 13. Utility composite curve with two utilities.

Table 4. Summary of results/Summary of data analysis

	Base case	Target	Optimized
Heating cost [$/year]	34,364	27,587	28,535
Heating load [kW]	46.47	46.30	46.47
Cooling load [kW]	0.18	0.00	0.18
Area [m^2]	4.917	8.51	7.140
New area [m^2]	-	-	3.104
Shell	4	10	6
New shell	-	-	3
New area cost [$]	-	-	32,470
Savings [$/year]	-	-	5,829
Payback [year]	-	-	5.574

pressure steam, and another heat exchanger is placed in front of the reheater to reduce the thermal load of the TEG regenerator reheater and to supply heat from the [Regen Bttms]-[Lean from L/R] flow. To examine the improvement in thermal performance due to the modifications, the target (ΔT_{min}=8.5 °C) data are compared with an existing process system (shown in Fig. 4). The energy cost and

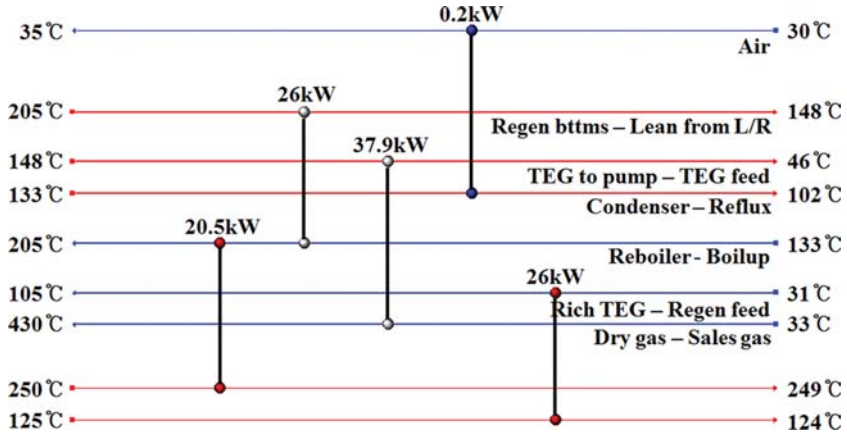

Fig. 14. Grid diagram of suggested model.

initial investment cost were evaluated, and the results are summarized in Table 4. While the annual operating cost for moisture removal from an LNG output of 100 TPD was estimated to be approximately $34,364, the annual operating cost was $28,535 when heat was supplied to the low-level section using low-pressure steam (125 °C, 500 kPa), as shown in Fig. 14. Therefore, the suggested modification brought about a savings of approximately $5,829 (17%) compared to existing configurations of the utilities.

CONCLUSION

A pinch analysis was modeled and performed for the moisture removal process from natural gas in an LNG plant processing system, and the process improvement was investigated by considering the energy target and economic efficiency.

The hot streams and cold streams in the dehydration process and the utility system were properly defined. Based on the static process model and the resulting composite curve data for the moisture removal process and the utility system, the differences between the heat exchange temperatures were confirmed to be reduced by using several levels of low-level utilities.

When the energy target temperature was set closer to ΔT_{min}= 8.5 °C in the moisture removal process and low-pressure steam was added to the glycol supply and regeneration systems, approximately 61% (102.9 MJ/h) of the total heat supply could be replaced with low-grade steam. In this case, the annual energy cost was reduced by approximately 17%.

In the future, various influencing factors, such as a commercial-scale moisture removal process, the physical properties of the supplied natural gas, and the heat exchanger type, will also be considered in a comprehensive manner.

ACKNOWLEDGEMENTS

This research was supported by a grant (19IFIP-B089072-06) from the Ministry of Land Transportation Technology Business Support Program, funded by the Ministry of Land, Infrastructure and Transport of the Korean government.

REFERENCES

1. S. Eggleston, L. Buendia, K. Wa, T. Ngara and K. Tanabe, IPCC guidelines for national greenhouse gas inventories, IPCC (2006).
2. G. C. Yeo, *NICE*, **28**(1), 32 (2010).
3. T. V. Nguyen, L. Pierobon and B. Elmegaard, *Energy*, **62**, 23 (2013).
4. C. Bengtsson, R. Nordman and T. Berntsson, *Appl. Therm. Eng.*, **22**(9), 1069 (2002).
5. I. Quesada and I. E. Grossmann, *Comput. Chem. Eng.*, **19**(12), 1219 (1995).
6. B. Linnhoff, *Comput. Chem. Eng.*, **3**, 295 (1979).
7. M. Ebrahim and A. Kawari, *Appl. Energy*, **65**(1), 45 (2000).
8. J. Geldermann, M. Treitz and O. Rentz, *Eur. J. Opera. Res.*, **171**, 1020 (2006).
9. H. W. Ryu, N. G. Kim, S. O. Kang, M. Oh and C. H. Lee, *Korean J. Chem. Eng.*, **36**(8), 1226 (2019).
10. R. Smith, M. Jobson and L. Chen, *Appl. Therm. Eng.*, **30**(16), 2281 (2010).
11. M. Ebrahim and A. Kawari, *Appl. Energy*, **65**(1), 45 (2000).
12. D. Song, Y. G. Yoon and C. J. Lee, *Korean J. Chem. Eng.*, **35**(12), 2348 (2018).
13. S. G. Yoon, J. Lee and S. Park, *Appl. Therm. Eng.*, **27**(5), 886 (2007).
14. C. Tuan, Y. L. Yeh, L. F. Hsu and T. C. Chen, *Korean J. Chem. Eng.*, **29**(3), 341 (2012).
15. S. Mokhatab, W. Poe and J. Speight, *Handbook of natural gas transmission and processing*, 3rd Ed., Gulf Professional Publishing, Oxford (2015).
16. D. Y. Peng, and D. B. Robinson, *Ind. Eng. Chem. Fundam.*, **15**(1), 59 (1976).
17. K. S. Pitzer, *Thermodynamic*, 3rd Ed., McGraw-Hill, New York (1955).
18. I. C. Kemp, *Pinch analysis and process integration: a user guide on process integration for the efficient use of energy*, 2nd Ed., Elsevier Publication, Oxford (2008).
19. Aspen energy analyzer: user guide, Aspen Technology Inc., Cambridge (2011)
20. Basic design package for LNG test bed train No. 1, GS E&C, Seoul (2010).